

Contribution from the Department of Chemistry,  
North Carolina State University, Raleigh, North Carolina 27607

## Mössbauer Study of Stibonic and Stibinic Acids: Structural Implications from Orbital Population Analysis

L. H. BOWEN\* and G. G. LONG

Received July 13, 1977

A series of amorphous stibonic acids,  $\text{RSbO}_3\text{H}_2$ , one stibinic acid,  $(p\text{-CH}_3\text{Ph})_2\text{SbO}_2\text{H}$ , and  $\text{Ph}_3\text{SbO}$  have been studied by  $^{121}\text{Sb}$  Mössbauer spectroscopy. The isomer shift,  $\delta$ , decreases almost linearly with increasing number of R groups. Both the stibonic and stibinic acids have appreciable values of  $\eta$  as well as quadrupole coupling constants on the order of  $\pm 10 \text{ mm s}^{-1}$ . Using an additive model to obtain orbital populations along the Sb ligand bonds for various assumed geometries, it is concluded that the typical Sb site in the amorphous acids has approximately trigonal-bipyramidal geometry with bridging oxygens in apical positions. The orbital population along the equatorial Sb-OH bond,  $\sigma_{\text{OH}}$ , is appreciably larger than the apical  $\sigma_{\text{OH}}$  in  $\text{Ph}_4\text{SbOH}$ .

### Introduction

In an earlier paper,<sup>1</sup> we have developed a method for using Mössbauer isomer shifts and quadrupole splittings to obtain electron populations in the hybrid atomic orbitals used by Sb(V) to form bonds. The method was applied primarily to compounds of the type  $\text{Ph}_{5-x}\text{SbCl}_x$ ,  $x = 1-4$ . It was assumed that a localized molecular orbital  $\phi_L$  along a given Sb-L bond was a linear combination of an Sb hybrid atomic orbital  $h_L$  and a ligand orbital  $\chi_L$ ,  $\phi_L = c_1 h_L + c_2 \chi_L$ , where  $h_L$  is fixed by the Sb geometry. The Sb orbital population in  $h_L$  is then  $\sigma_L = 2c_1^2$ . These results indicated the method was of general applicability to organoantimony(V) halides at least. Concerning bonding in these compounds, a marked trend was observed in the population along the Sb-Ph bonds,  $\sigma_{\text{Ph}}$  increasing as the number of electronegative groups bonded to Sb increased. Also the relative 5s character of the apical and equatorial bonds in the trigonal-bipyramidal structures was shown to be about equal.

In the present work we apply this method to organoantimony(V) compounds containing oxygen. A distinct difference from the previous work is that little structural information is available on the stibonic,  $\text{RSbO}_3\text{H}_2$ , and stibinic acids,  $\text{R}_2\text{SbO}_2\text{H}$ , as these compounds are amorphous, insoluble, and presumably polymeric materials.<sup>2</sup> Thus, the method cannot be expected to give orbital populations with even the limited precision of the earlier study. However, it will be shown that certain reasonable assumptions about the orbital populations can lead to structural information about the average Sb site in these amorphous materials. The application of Mössbauer spectroscopy to amorphous materials is proving to be one of its more useful applications,<sup>3</sup> as it is primarily the short-range order which determines the Mössbauer parameters of a solid. The orbital population method, at least in the present case, enables a more detailed interpretation of the structural implications of the Mössbauer parameters.

### Experimental Section

Our cryostat, spectral procedures, and data analysis have been described.<sup>1,4</sup> The 4 K spectra were obtained with a  $\text{Ni}_{21}\text{Sn}_2\text{B}_6(^{121}\text{Sb})$  source and the conversion  $1.65 \text{ mm s}^{-1}$  added to obtain the isomer shift relative to  $\text{InSb}$ .<sup>1</sup> Mössbauer parameters obtained in the present work are given in Table I. For convenient reference several Sb(V) oxygen compounds reported previously have also been listed. An interesting feature of the present series is the large value of  $\eta$  obtained in many cases,  $\eta$  being the quadrupole asymmetry parameter. For the  $^{57}\text{Fe}$  transition of  $^{121}\text{Sb}$ ,  $\eta$  cannot be obtained with precision due to overlap of the various line components. However  $\eta = 0$  gives a very unsymmetrical spectrum (unlike the  $^{57}\text{Fe}$  case) and as  $\eta \rightarrow 1$  the spectrum becomes more symmetrical.<sup>8</sup>

A typical spectrum is shown in Figure 1. It should be noted that alternate fits to the data have been considered. The curve is much too broad and flat to be a single peak, even if some line broadening

Table I. Mössbauer Parameters of Sb(V) Compounds<sup>a</sup>

Compd	Intensity, %	$\Gamma$ , $\pm 0.1 \text{ mm s}^{-1}$	$\delta$ , $\pm 0.05 \text{ mm s}^{-1}$	$e^2qQ$ , $\pm 1 \text{ mm s}^{-1}$	$\eta$ , $\pm 0.2$
$\text{Sb}_2\text{O}_4^b$		3.5	8.78		
$\text{PhSbO}_3\text{H}_2$	32	2.9	6.77	9.5	0.7
$m\text{-CH}_3\text{PhSbO}_3\text{H}_2$	40	2.8	6.79	8.7	0.9
$p\text{-CH}_3\text{PhSbO}_3\text{H}_2$	34	2.9	6.85	9.8	0.7
$p\text{-CH}_3\text{O}_2\text{CPhSbO}_3\text{H}_2$	40	2.8	6.80	10.7	0.6
$(p\text{-CH}_3\text{Ph})_2\text{SbO}_2\text{H}$	36	2.8	6.01	-9.5	0.9
$\text{Ph}_3\text{SbO}$	38	2.8	5.27	-10.6	0
$\text{Ph}_3\text{Sb}(\text{OCOCH}_3)_2^c$		2.8	3.7	-21.8	<0.3
$\text{Ph}_4\text{SbOH}^c$		2.9	4.4	-5.3	0

<sup>a</sup> Isomer shifts,  $\delta$ , relative to  $\text{InSb}$ . Line width,  $\Gamma$ , at half-maximum. All new samples contained about  $10 \text{ mg of Sb cm}^{-2}$  and were measured at 4 K. <sup>b</sup> Reference 5. Absorber and source at 77 K. Sb(V) peak only. <sup>c</sup> Reference 6. Absorber at 9 K, source at 77 K. Isomer shift converted from  $\text{BaSnO}_3$  by adding  $8.5 \text{ mm s}^{-1}$  (ref 7).

due to the amorphous nature of the material is allowed. If the data are assumed to indicate two distinct sites, the fit is reasonably good but the two lines are separated in isomer shift by about  $2 \text{ mm s}^{-1}$  and, while somewhat broader than known single-line spectra, the two lines would each have almost no quadrupole splitting. This would indicate two very symmetrical sites for Sb of almost (but not exactly) equal intensity, each of which is quite different in ligand electronegativity. The stoichiometry makes this highly unlikely. The fit to one site with  $e^2qQ$  and  $\eta$  gives similar line width to spectra of known structures and isomer shifts varying in reasonable fashion with the number of organic groups per Sb. The line width indicates all Sb sites are similar in this material.

Powder x-ray diffraction patterns were taken of all the new samples reported in Table I. Of these, only  $\text{Ph}_3\text{SbO}$  showed any sign of crystallinity. Its powder pattern was quite complex but indicated a highly crystalline material.

These compounds have been previously described and were prepared by known methods. The crude stibonic and stibinic acids<sup>9</sup> were converted to the corresponding pyridinium arylchloroantimonates for recrystallization from which the free acids were regenerated. The triphenylantimony oxide was prepared by refluxing tetraphenylstibonium hydroxide in xylene as given by Briles and McEwen<sup>10</sup> and had a melting point of  $221^\circ\text{C}$ . Antimony was determined for all of the preparations and was found to be within  $\pm 0.1\%$  of theoretical; in addition C and H were determined for triphenylantimony oxide. Anal. Calcd: C, 58.58; H, 4.10. Found: C, 58.79; H, 4.17.

### Results and Conclusions

Since the stibonic and stibinic acids are polymeric, oxygen bridging between antimonys is likely an important feature of the geometry. The Mössbauer data suggest each compound has only one Sb site or at least in all sites the local symmetry is similar. The purpose of our analysis is to find a regular geometry to describe this site, one which gives reasonable

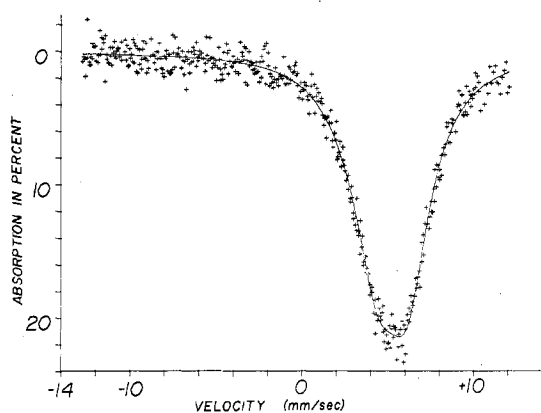


**Figure 1.** Mössbauer spectrum of  $p\text{-CH}_3\text{PhSbO}_3\text{H}_2$  at 4 K fit with both  $e^2qQ$  and  $\eta$ . The parameters used are given in Table I except the velocity scale is relative to the  $\text{Ni}_{21}\text{Sn}_2\text{B}_6$  source,  $1.65 \text{ mm s}^{-1}$  more positive than InSb.

orbital populations along the antimony–ligand bonds. The two geometries we consider are octahedral and trigonal bipyramidal. The appropriate hybrid orbitals and their contributions to the total 5s electron density,  $n_s$ , and 5p electron density,  $n_p$ , have been given.<sup>1</sup> The components of the field gradient tensor can be expressed in terms of the orbital populations  $\sigma_i$  and a scale factor  $K = e^2c|Q|\langle r^{-3} \rangle_p/E_\gamma$ , taken as  $37 \text{ mm s}^{-1}$  as justified earlier.<sup>1</sup> The acids have three different  $\sigma$ 's:  $\sigma_R$  along the organic ligand bond,  $\sigma_{\text{OH}}$ , and  $\sigma_{\text{OB}}$  along the oxygen bridging bond. For an assumed geometry the nonzero values of  $e^2qQ$  and  $\eta$  allow two of the  $\sigma$ 's to be expressed in terms of the third. The isomer shift calibration<sup>1</sup>

$$\delta = 17.3 - n_s(23.3 - 2.0n_p) \quad (1)$$

then allows assignment of values to all three  $\sigma$ 's. We have assumed here, as discussed earlier,<sup>1</sup> that the s–d mixing parameter  $\cos^2 \theta = 0.4$  for trigonal-bipyramidal geometry, which gives equal contributions to  $n_s$  from apical and equatorial orbitals. Any other choice would affect the magnitude of the  $\sigma$ 's but not their differences, which are determined by  $e^2qQ$  and  $\eta$ .

It should be noted that while chemical intuition requires  $\sigma_R$  to be greater than  $\sigma_{\text{OH}}$  or  $\sigma_{\text{OB}}$ , the relative values of these latter two are not so clear. In the halogen case,<sup>1</sup> bridging Cl had a larger  $\sigma$  and a smaller effective scale factor  $K'/K = 0.7$ . However, the bridging Cl–Sb bond distance is appreciably longer than nonbridging in  $\text{Ph}_2\text{SbCl}_3$ .<sup>11</sup> The O–Sb bond distance in both  $\text{Ph}_4\text{SbOH}$  and  $\text{Ph}_4\text{SbOCH}_3$  is  $2.06 \text{ \AA}$ ,<sup>12,13</sup> just slightly longer than in a typical bridged inorganic oxide such as  $\text{Sb}_2\text{O}_4$ , which has  $1.96\text{--}1.99 \text{ \AA}$  for O–Sb(V).<sup>14</sup> It should be noted that since oxygen is divalent, it is bridging in Sb–O–H as well as in Sb–O–Sb and really different from Cl in this regard. Thus, another objective of the analysis is to clarify the relative values of  $\sigma_{\text{OH}}$  and  $\sigma_{\text{OB}}$ .

The compound  $\text{Ph}_4\text{SbOH}$  is known to have trigonal-bipyramidal geometry about Sb,<sup>12</sup> with the OH in an apical position. The apical C–Sb bond distance is slightly longer than the equatorial. Since these two populations cannot be separately determined, we assume an average  $\sigma_R$  and obtain

$$V_{zz} = -e^2qQ = (2/5)K(\sigma_R - \sigma_{\text{OH}})$$

$$n_s = (1/5)\sigma_{\text{OH}} + (4/5)\sigma_R \quad (2)$$

$$n_p = (1/2)\sigma_{\text{OH}} + (5/2)\sigma_R$$

The measured values for  $e^2qQ$  and  $\delta^6$  (see Table I) give, from eq 2 and 1 above,  $\sigma_R = 0.74$  and  $\sigma_{\text{OH}} = 0.38$ . In comparison  $\text{Ph}_4\text{SbCl}$  gave  $\sigma_R = 0.83$ ,  $\sigma_{\text{Cl}} = 0.38$ .<sup>1</sup> The large increase in  $\sigma_R$  upon substituting a second electronegative group in  $\text{Ph}_3\text{SbCl}_2$  ( $\sigma_R = 1.07$ )<sup>1</sup> is observed also in the trigonal-

**Table II.** Orbital Populations in Sb(V) Oxo Compounds According to Trigonal-Bipyramidal Geometry (See Figure 3)

Compd	$\sigma_R$	$\sigma_{\text{OH}}$	$\sigma_{\text{OB}}$
$\text{Ph}_4\text{SbOH}$	0.74	0.38	
$\text{Ph}_3\text{SbO}$	0.76		0.40
$(p\text{-CH}_3\text{Ph})_2\text{SbO}_2\text{H}$	0.80	0.51	0.38
$\text{PhSbO}_3\text{H}_2$	0.89	0.52	0.37
$p\text{-CH}_3\text{PhSbO}_3\text{H}_2$	0.89	0.51	0.36
$m\text{-CH}_3\text{PhSbO}_3\text{H}_2$	0.84	0.53	0.35
$p\text{-CH}_3\text{O}_2\text{CPhSbO}_3\text{H}_2 \cdot \text{H}_2\text{O}$	0.92	0.49	0.35

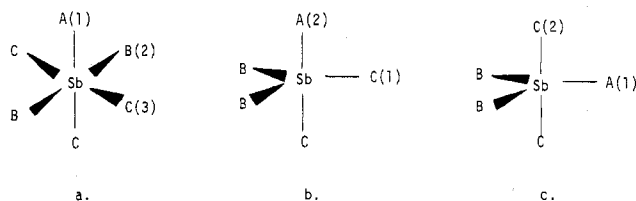


**Figure 2.** Geometries of general interest: (a) octahedral, (b) and (c) trigonal bipyramidal.

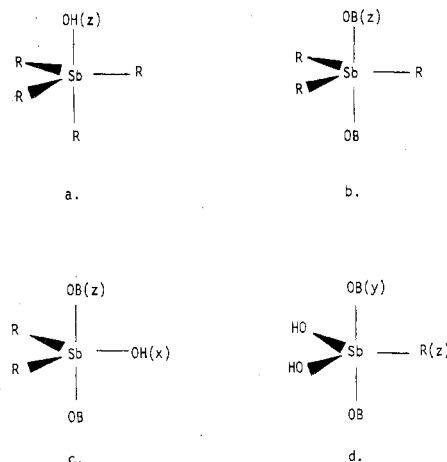


**Figure 3.** Assumed geometry for Sb(V) oxo compounds (see Table II): (a)  $\text{Ph}_4\text{SbOH}$ , (b)  $\text{Ph}_3\text{SbO}$ , (c)  $\text{R}_2\text{SbO}_2\text{H}$ , (d)  $\text{RSbO}_3\text{H}_2$ .

bipyramidal  $\text{Ph}_3\text{Sb}(\text{OCOME})_2$ ,<sup>6</sup> which gives  $\sigma_R = 1.02$ ,  $\sigma_{\text{OCOME}} = 0.29$ , calculated in a similar manner.

The compound  $\text{Ph}_3\text{SbO}$ , whose structure is not known, has very different Mössbauer parameters from the latter compound, its  $e^2qQ$  being considerably smaller and  $\delta$  more positive. If its structure is also assumed to be trigonal bipyramidal, with bridging oxygens in the apical positions, then  $\sigma_{\text{OB}} - \sigma_R$  must be the same as  $\sigma_{\text{OH}} - \sigma_R$  in  $\text{Ph}_4\text{SbOH}$  due to the fact that  $e^2qQ$  is almost exactly twice as large. The isomer shift then gives absolute values of  $\sigma_R = 0.76$ ,  $\sigma_{\text{OB}} = 0.40$ . The orbital population results are tabulated in Table II. It should be pointed out that no octahedral configuration with three R and three O bridges will satisfy the experimentally observed negative  $e^2qQ$  and zero  $\eta$ , and the proposed trigonal bipyramid seems the only simple one to fit the data. Thus, unlike the corresponding halides or  $\text{Ph}_3\text{Sb}(\text{OCOME})_2$ , the  $\sigma$ 's hardly differ between  $\text{Ph}_4\text{SbOH}$  and  $\text{Ph}_3\text{SbO}$ .

There is an almost linear trend of  $\delta$  with number of R groups in the series  $\text{Ph}_4\text{SbOH}$ ,  $\text{Ph}_3\text{SbO}$ ,  $\text{R}_2\text{SbO}_2\text{H}$ , and  $\text{RSbO}_3\text{H}_2$ . This relationship suggests that the amorphous acids have a trigonal-bipyramidal Sb site also, although with bridging oxygens, octahedral geometry cannot be ruled out on this basis alone. There is no simple trend in  $e^2qQ$ , but both stibinic and stibonic acids have large values of  $\eta$ .

Consider first the one stibinic acid studied, ( $p\text{-CH}_3\text{Ph}$ )<sub>2</sub>SbO<sub>2</sub>H. About each Sb we assume two R groups,

one OH, and the rest bridging oxygens OB. Possible structures are shown in Figure 2 (A being OH) and the field gradient components are given in the Appendix for each. Experimentally, in units of  $(2/5)K$ ,  $V_{zz} = +0.64$  and  $\eta V_{zz} = V_{xx} - V_{yy} = 0.58$ . The positive  $V_{zz}$  requires electronegative groups along the  $z$  axis, while the large  $\eta$  indicates the two R groups have their largest component along the  $y$  axis. Thus for the octahedral structure Figure 2a, B is the organic R group and axis (2) is the  $y$  axis. For structure 2b, B must be the R group (as the two C's are on separate axes). For structure 2c, B or C could be R. The main criterion for a reasonable fit is that  $\sigma_R > \sigma_{OH} \sim \sigma_{OB}$ . The two experimental numbers give two  $\sigma$ 's in terms of the third.

For the octahedral structure 2a with (2) as  $y$  and (1) as  $z$ :  $\sigma_R = \sigma_{OH} + 0.64$  and  $\sigma_{OB} = \sigma_{OH} + 0.45$ . For structure 2b the best choice for the  $z$  axis is (2), which gives  $\sigma_R = \sigma_{OH} + 0.54$ ,  $\sigma_{OB} = \sigma_{OH} + 0.25$ . For structure 2c with B = R and (2) as the  $z$  axis,  $\sigma_R = \sigma_{OB} + 0.42$ ,  $\sigma_{OH} = \sigma_{OB} + 0.13$ . If, however, C = R and (1) is  $z$ ,  $\sigma_R = \sigma_{OH} + 0.53$  and  $\sigma_{OB} = \sigma_{OH} + 0.34$ . Using the fit which minimizes the difference between  $\sigma_{OH}$  and  $\sigma_{OB}$  gives a marked preference to structure 2c with B = R and (2) as  $z$ . It could be that part of the field gradient interaction comes from deviation from regular geometry, but since x-ray structure determination cannot be carried out in these amorphous materials, the geometry is unknown. It is not proposed that the Sb sites are truly as in structure 2c, only that the actual sites look more like that than any other simple configuration. It is noted that the bridging oxygens in the preferred structure are on opposite sides of Sb, which is geometrically reasonable. Substituting for  $n_s$  and  $n_p$  in terms of  $\sigma_{OB}$ , the isomer shift equation (1) can be used to obtain values of all three  $\sigma$ 's as tabulated in Table II. While  $\sigma_{OB}$  is about the same as in  $\text{Ph}_3\text{SbO}$ ,  $\sigma_{OH}$  is considerably larger than in  $\text{Ph}_2\text{SbOH}$ . This difference between equatorial and apical OH is independent of the  $s$ - $d$  mixing parameter and indicates a less ionic Sb-OH bond in the equatorial plane.

The various stibonic acids studied all have similar Mössbauer parameters: positive  $e^2qQ$ , large  $\eta$ , and  $\delta$  more positive than for the stibinic acid. For illustration we take  $\text{PhSbO}_3\text{H}_2$  with, in units of  $(2/5)K$ ,  $V_{zz} = -0.64$  and  $\eta V_{zz} = -0.45$ . We again choose axes for the field gradient to make  $\sigma_R > \sigma_{OH} \sim \sigma_{OB}$ . In each general structure in Figure 2 this requires A = Ph and the  $z$  axis to lie on the Sb-Ph bond. In the octahedral structure 2a B must be OH, but it is impossible in structure 2b or 2c to determine which is OH, B, or C or which is larger  $\sigma_{OH}$  or  $\sigma_{OB}$ . Thus we pick B = OH and  $\sigma_{OH} > \sigma_{OB}$ , to be in agreement with  $(p\text{-CH}_3\text{Ph})_2\text{SbO}_2\text{H}$  above. The appropriate field gradient relations (see Appendix) give for structure 2a,  $\sigma_{OH} = \sigma_{OB} + 0.15$ ,  $\sigma_{Ph} = \sigma_{OB} + 0.79$ . For 2b  $\sigma_{OH} = \sigma_{OB} + 0.22$  and  $\sigma_{Ph} = \sigma_{OB} + 0.94$ . For 2c  $\sigma_{OH} = \sigma_{OB} + 0.15$  and  $\sigma_{Ph} = \sigma_{OB} + 0.52$ . In 2a and 2b  $\sigma_{Ph}$  appears much larger than  $\sigma_{OB}$  compared to the previous compounds, and therefore 2c is the preferred geometry. It is gratifying that again the trigonal-bipyramidal structure with bridging oxygens along the apical bonds gives the most consistent set of  $\sigma$ 's. The isomer shift can be used to calculate all three  $\sigma$ 's, as listed in Table II. The one hydrated stibonic acid studied,  $p\text{-CH}_3\text{O}_2\text{CPhSbO}_3\text{H}_2 \cdot \text{H}_2\text{O}$ , has Mössbauer parameters very similar to those of the others, indicating the water does not markedly alter the local environment about Sb.

Looking at the overall trend in orbital populations in Table II,  $\sigma_R$  increases slightly with increased substitution of electronegative groups but not nearly as much as the halogen series. Among the substituted stibonic acids, the  $\sigma$ 's probably should be considered constant within experimental error. The bridging oxygens, assumed to be apical, have  $\sigma_{OB}$  in the range 0.35–0.40, similar to the apical  $\sigma_{OH}$  in  $\text{Ph}_4\text{SbOH}$  and to  $\sigma_{OB}$  in the octahedral  $\text{Sb}_2\text{O}_4$ , which is calculated from the isomer

shift<sup>5</sup> (Table I) as  $\sigma_{OB} = 0.41$ . However, the orbital population  $\sigma_{OH}$  in an equatorial position is appreciably larger at  $\sim 0.52$ . It should be mentioned that in five-coordinate Sn(IV) compounds, the equatorial  $\sigma$  tends to be lower than apical for a given ligand,<sup>15</sup> although OH as ligand was not studied.

In summary, a description of the average Sb site geometry in the amorphous stibonic and stibinic acids consistent with their Mössbauer parameters has bridging oxygens on opposite sides of Sb and approximately trigonal-bipyramidal geometry, with either OH or R groups in the equatorial plane. The orbital population analysis favors this arrangement over alternate octahedral or trigonal-bipyramidal geometries. The equatorial Sb-OH bonds are more covalent than apical Sb-OH or Sb-O-Sb. This conclusion is in agreement with the relative acidity of the stibonic and stibinic acids<sup>2</sup> compared to the basic OH in  $\text{Ph}_4\text{SbOH}$ . It would be of considerable interest to have a structure determination of the crystalline  $\text{Ph}_3\text{SbO}$ , since agreement with our proposed structure would make application of the orbital method to amorphous compounds more certain.

**Acknowledgment.** This work was supported in part by the National Science Foundation under Grant GP-33516. The assistance of S. W. Hedges in obtaining the Mössbauer spectra is gratefully acknowledged.

## Appendix

In Figure 2 are shown the geometries we consider for both stibonic acids (A = R group) and stibinic (A = OH). Since  $\eta$  is nonzero and since we do not know in advance which is the  $z$  axis, we need to consider all three components of the field gradient tensor. The term  $\eta V_{zz} = V_{xx} - V_{yy}$ , so that given the  $z$  axis,  $x$  and  $y$  can be interchanged to make  $\eta$  positive. For the additive model, in units of  $(2/5)K$ , the components for these geometries are the following:

$$\begin{aligned} \text{(a)} \quad & V_{11} = -\sigma_A + \sigma_B & V_{22} - V_{33} = -3\sigma_B + 3\sigma_C \\ & V_{22} = 1/2\sigma_A - 2\sigma_B + 3/2\sigma_C & V_{33} - V_{11} = 3/2\sigma_A - 3/2\sigma_C \\ & V_{33} = 1/2\sigma_A + \sigma_B - 3/2\sigma_C & V_{11} - V_{22} = -3/2\sigma_A + 3\sigma_B - 3/2\sigma_C \\ \text{(b)} \quad & V_{11} = 1/2\sigma_A + 1/3\sigma_B - 5/6\sigma_C & V_{22} - V_{33} = -3/2\sigma_A + 3\sigma_B - 3/2\sigma_C \\ & V_{22} = -\sigma_A + 4/3\sigma_B - 1/3\sigma_C & V_{33} - V_{11} = -2\sigma_B + 2\sigma_C \\ & V_{33} = 1/2\sigma_A - 5/3\sigma_B + 7/6\sigma_C & V_{11} - V_{22} = 3/2\sigma_A - \sigma_B - 1/2\sigma_C \\ \text{(c)} \quad & V_{11} = -4/3\sigma_A + 1/3\sigma_B + \sigma_C & V_{22} - V_{33} = 3\sigma_B - 3\sigma_C \\ & V_{22} = 2/3\sigma_A + 4/3\sigma_B - 2\sigma_C & V_{33} - V_{11} = 2\sigma_A - 2\sigma_B \\ & V_{33} = 2/3\sigma_A - 5/3\sigma_B + \sigma_C & V_{11} - V_{22} = -2\sigma_A - \sigma_B + 3\sigma_C \end{aligned}$$

Because of equal number of B and C, structures (b) and (c) are the only unique trigonal bipyramids. In structure (a) to maximize the difference between axes (2) and (3) we place both B's on one axis. The alternative with one B on axis (3) would have  $\eta = 0$ . The alternative with one B on axis (1) would have smaller  $\eta$  than the structure shown.

**Registry No.**  $\text{PhSbO}_3\text{H}_2$ , 535-46-6;  $m\text{-CH}_3\text{PhSbO}_3\text{H}_2$ , 65275-99-2;  $p\text{-CH}_3\text{PhSbO}_3\text{H}_2$ , 5450-68-0;  $p\text{-CH}_3\text{O}_2\text{CPhSbO}_3\text{H}_2$ , 65275-98-1;  $(p\text{-CH}_3\text{Ph})_2\text{SbO}_2\text{H}$ , 5430-43-3;  $\text{Ph}_3\text{SbO}$ , 4756-75-6;  $\text{Ph}_4\text{SbOH}$ , 19638-16-5.

## References and Notes

- L. H. Bowen and G. G. Long, *Inorg. Chem.*, **15**, 1039 (1976).
- G. O. Doak and L. D. Freedman, "Organometallic Compounds of Arsenic, Antimony and Bismuth", Wiley-Interscience, New York, N.Y., 1970, pp 291-293.
- J. G. Stevens and L. H. Bowen, *Anal. Chem.*, **48**, 232R (1976).
- L. H. Bowen, P. E. Garrou, and G. G. Long, *J. Inorg. Nucl. Chem.*, **33**, 953 (1971).
- D. J. Stewart, O. Knop, C. Ayasse, and F. W. D. Woodhams, *Can. J. Chem.*, **50**, 690 (1972).
- J. N. R. Ruddick, J. R. Sams, and J. C. Scott, *Inorg. Chem.*, **13**, 1503 (1974).
- L. H. Bowen in "Mössbauer Effect Data Index, 1972", J. G. Stevens and V. E. Stevens, Ed., IFI/Plenum, New York, N.Y., 1973, p 71.
- L. H. Bowen, G. G. Long, J. G. Stevens, N. C. Campbell, and T. B. Brill, *Inorg. Chem.*, **13**, 1787 (1974).
- G. O. Doak and H. G. Steinman, *J. Am. Chem. Soc.*, **68**, 1987 (1946).

- (10) G. H. Briles and W. E. McEwen, *Tetrahedron Lett.*, **43**, 5299 (1966).  
 (11) J. Bordner, G. O. Doak, and J. R. Peters, Jr., *J. Am. Chem. Soc.*, **96**, 6763 (1974).  
 (12) A. C. Beauchamp, M. J. Bennett, and F. A. Cotton, *J. Am. Chem. Soc.*, **91**, 297 (1969).  
 (13) K. Shen, W. E. McEwen, S. J. LaPlaca, W. C. Hamilton, and A. P. Wolf, *J. Am. Chem. Soc.*, **90**, 1718 (1968).  
 (14) D. Rogers and A. C. Skapski, *Proc. Chem. Soc., London*, 400 (1964).  
 (15) G. M. Bancroft, V. G. K. Das, T. K. Sham, and M. G. Clark, *J. Chem. Soc., Dalton Trans.*, 643 (1976).

Contribution from the Department of Chemistry,  
 The University of Oklahoma, Norman, Oklahoma 73019

## High-Pressure Reactions of Small Covalent Molecules. 10. The Reaction of PF<sub>3</sub> with H<sub>2</sub>S and SO<sub>2</sub><sup>1</sup>

ARNULF P. HAGEN\* and BILL W. CALLAWAY

Received July 21, 1977

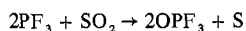
Phosphorus trifluoride reacts with sulfur dioxide and hydrogen sulfide at increased pressure. The reaction yields within 24 h are greatly influenced by pressure. The sulfur dioxide reaction forms sulfur and OPF<sub>3</sub> in a 4% yield at 150 °C (670 atm) and 84% yield at 150 °C (4000 atm). The hydrogen sulfide interaction leads to a 3% yield of SPF<sub>3</sub> and hydrogen at 200 °C (1350 atm) and a 35% yield at 200 °C (4000 atm). When longer reaction times are used, both reactions become nearly quantitative which indicates pressure is changing the rate of the reaction. This rate increase supports a mechanism in which the rate-determining step involves a bond formation rather than an initial decomposition of sulfur dioxide or hydrogen sulfide.

Phosphorus trifluoride has been shown to react at increased pressure with sulfides and oxides.<sup>2-4</sup> For example, when PF<sub>3</sub> was combined with nickel(II) oxide, Ni(PF<sub>3</sub>)<sub>4</sub> and OPF<sub>3</sub> were obtained, and when it reacted with carbon dioxide, OPF<sub>3</sub> and C or CO were formed. In this investigation, phosphorus trifluoride has been found to react with sulfur dioxide at 130 °C (3000 atm) and with hydrogen sulfide at 150 °C (4000 atm).

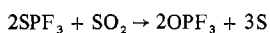
### Results and Discussion

Tables I and II summarize the experimental results when the samples are at the given conditions for 24 h. When the reaction period is longer, the quantity of material reacting increases and the reactions become essentially quantitative. Therefore the temperature and pressure changes are indicative of a rate change rather than a shift in equilibrium.

Sulfur dioxide is a well-known reducing agent. It has also been shown to oxidize (CH<sub>3</sub>)<sub>3</sub>P, (C<sub>6</sub>H<sub>5</sub>)<sub>3</sub>P, and PBr<sub>3</sub> at 185 °C in sealed silica tubes<sup>5</sup> and PCl<sub>3</sub> at 550 °C in a flow reactor.<sup>6</sup> In this study sulfur dioxide was found (Table I) to oxidize PF<sub>3</sub> at the minimum conditions 130 °C (3000 atm), 150 °C (670 atm), and 200 °C (335 atm) forming OPF<sub>3</sub> and sulfur:

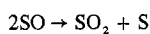
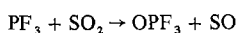


The lack of SPF<sub>3</sub> in all of the experiments was surprising, since phosphorus trifluoride readily reacts with sulfur at increased pressure<sup>2</sup> to form SPF<sub>3</sub>. The relative amounts of SO<sub>2</sub> and PF<sub>3</sub> were varied in experiments additional to those listed in Table I at pressures up to 4000 atm and at temperatures up to 500 °C in an attempt to isolate SPF<sub>3</sub>, but none was detected. It was found, however, at the mildest conditions where SO<sub>2</sub> and PF<sub>3</sub> interact, SPF<sub>3</sub> reacts with SO<sub>2</sub> to form OPF<sub>3</sub> and sulfur:



The lack of SPF<sub>3</sub> can therefore be explained if the rate of its reaction with SO<sub>2</sub> is greater than the rate of the reaction of PF<sub>3</sub> with sulfur.

It is reasonable to postulate that the overall reaction of PF<sub>3</sub> with SO<sub>2</sub> is a two-step process:



Since this reaction shows pressure dependence at relatively low

Table I. Sulfur Dioxide Reactions

P, atm	T, °C	% conversion <sup>a</sup>	Amt of reactants, mmol		Amt of material out, <sup>b</sup> mmol		
			PF <sub>3</sub>	SO <sub>2</sub>	PF <sub>3</sub>	SO <sub>2</sub>	OPF <sub>3</sub>
4000	100		0.81	0.75	0.80	0.74	
2000	130		0.81	0.82	0.80	0.80	
3000	130	14	0.83	0.84	0.71	0.78	0.12
4000	130	14	0.84	0.83	0.72	0.77	0.12
335	150		0.84	0.85	0.83	0.83	
670	150	4	0.91	0.89	0.87	0.87	0.04
1350	150	10	0.87	0.85	0.78	0.82	0.09
4000	150	84	0.83	0.84	0.13	0.49	0.70
335	200	6	0.82	0.82	0.77	0.80	0.05
2670	200	80	1.13	0.90	0.23	0.54	0.90
4000	200	88	0.82	0.86	0.10	0.48	0.72

<sup>a</sup> Based on mmol of PF<sub>3</sub> consumed. All experiments were for 24 h. <sup>b</sup> The amount of sulfur can be calculated from the material balance.

Table II. Hydrogen Sulfide Reactions

P, atm	T, °C	% conversion <sup>a</sup>	Amt of reactants, mmol		Amt of material out, <sup>b</sup> mmol		
			PF <sub>3</sub>	H <sub>2</sub> S	PF <sub>3</sub>	H <sub>2</sub> S	SPF <sub>3</sub>
2000	150		0.66	0.65	0.65	0.64	
4000	150	3	0.74	0.78	0.72	0.76	0.02
670	200		0.92	0.91	0.92	0.91	
1350	200	3	0.87	0.84	0.84	0.81	0.03
4000	200	35	0.75	0.77	0.49	0.49	0.28
670	500	32	1.11	1.19	0.75	0.85	0.34
3300	500	40	0.86	0.87	0.52	0.52	0.35

<sup>a</sup> Based on mmol of PF<sub>3</sub> consumed. All experiments were for 24 h. <sup>b</sup> The amount of hydrogen can be calculated from the material balance.

pressures and temperatures and since we have no evidence for any thermal decomposition of the SO<sub>2</sub> at the same conditions, it is most reasonable that the reaction takes place via a coordinated intermediate rather than by an initial thermal decomposition of sulfur dioxide.

The reactions with H<sub>2</sub>S are summarized in Table II. At conditions above 150 °C (4000 atm) or 200 °C (1350 atm) the reaction is

